Electronic Supplementary Material (ESI) for Polymer Chemistry.
This journal is © The Royal Society of Chemistry 2021

Copolymerization of Lactide, Epoxides and Carbon Dioxide: Highly Efficient Heterogeneous Ternary Catalyst System

Xiang Li[a], Ranlong Duan[b], Chenyang Hu[b], Xuan Pang[b]*, and Mingxiao Deng[a]*

[a] Institute of Chemistry, Northeast Normal University, Changchun, 130024, PR China.

[b] Key Laboratory of Polymer Ecomaterials, Changchun Institute of Applied Chemistry, Chinese Academy of Sciences, Changchun 130022, PR China.

Fig. S1 The different solubility of catalysts at room temperature (I: ZnGA; II: ZnGA at 60 ^{o}C after 0.5 hour; III: SalenCo^{III}; IV: SalenCo^{II}; V: SalenFe; VI: SalenAl).

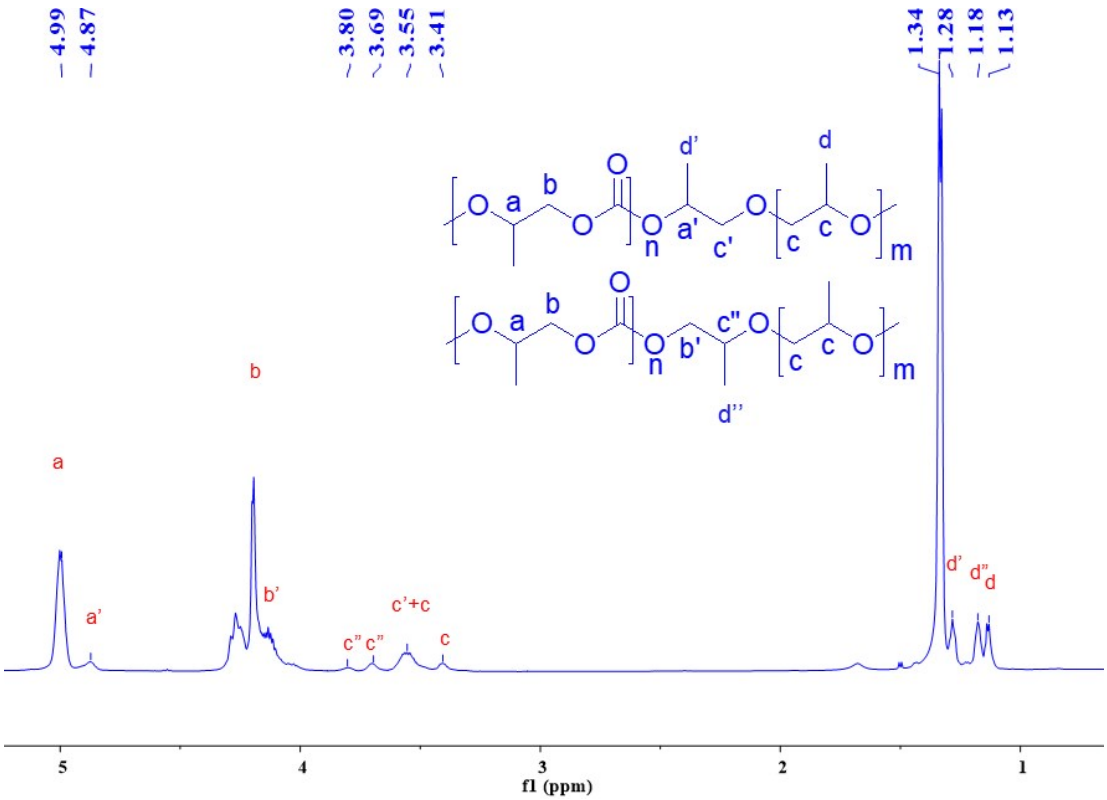

Fig. S2 The ^{1}H NMR spectrum of PPC_2 (Table 2, Entry 15), the PPO content is 7%.

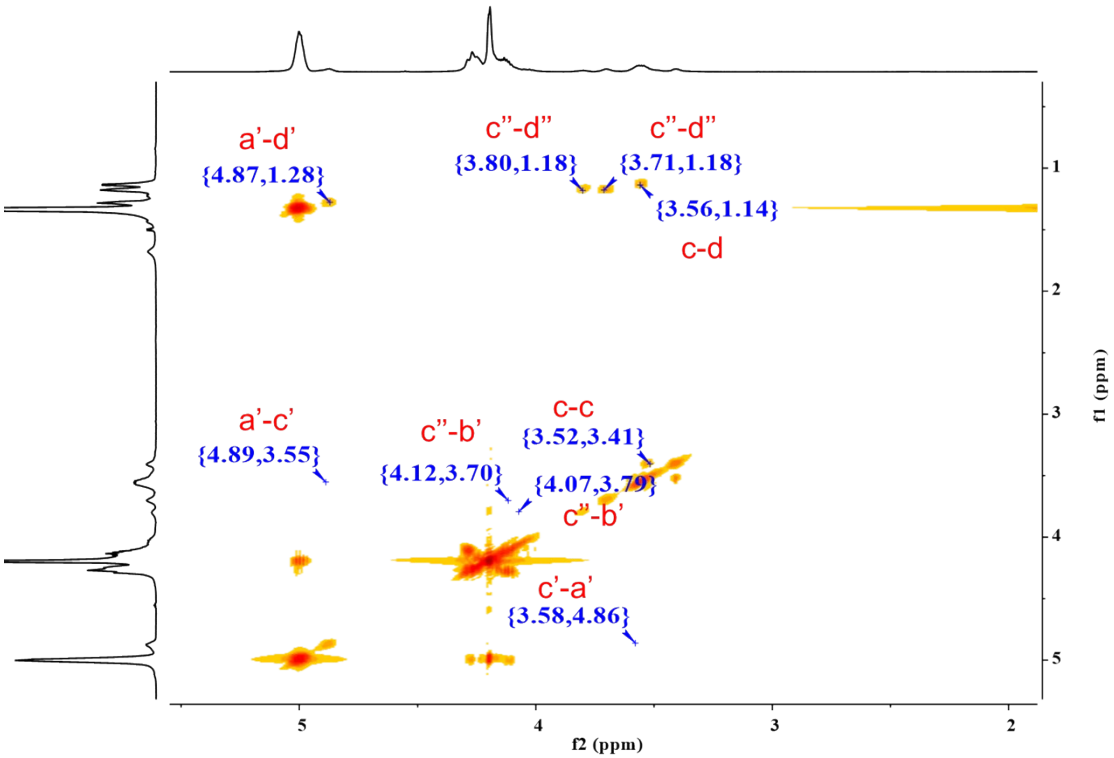

Fig. S3 The HH COSY NMR spectrum of PPC_2 (Table 1, Entry 4).

Table S1. The copolymerization of LLA, PO and CO_2.

Entry	1b[b]	**4**[b]	PPNCl[b]	PO[b]	LLA[b]	Time (h)	Conv.$_1$ (%)[c]	Sel.$_1$ (%)[c]	Conv.$_2$ (%)[c]	Sel.$_2$ (%)[c]	PLA% [c]
1	1	50	2	3500	500	1.5	9	52	18	1	38
2	1	50	2	3500	500	2.5	12	63	17	1	40
3	1	50	2	3500	500	3.5	18	82	41	1	44
4	1	50	2	3500	500	6	24	89	67	1	46

(a) The reactions were performed in 2 mL neat PO in 25 mL autoclave at 60 ^oC, 2 MPa CO_2. (b) Molar ratio. (c) Results based on the ^1H NMR spectroscopy. Con.$_1$ is for PO and Con.$_2$ is for LLA; Sel.1 is for polycarbonates over all converted PO; Sel.$_2$ is for PPO over all converted PO.

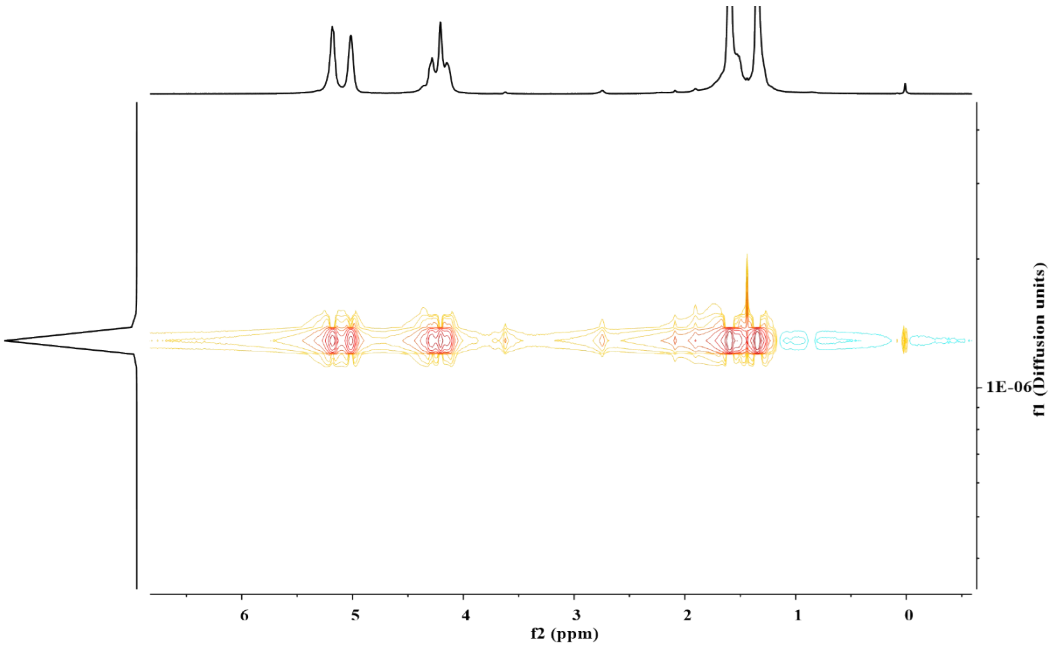

Fig.

Fig. S4 The ^{1}H DOSY NMR spectrum of $PLLAPC_2$.

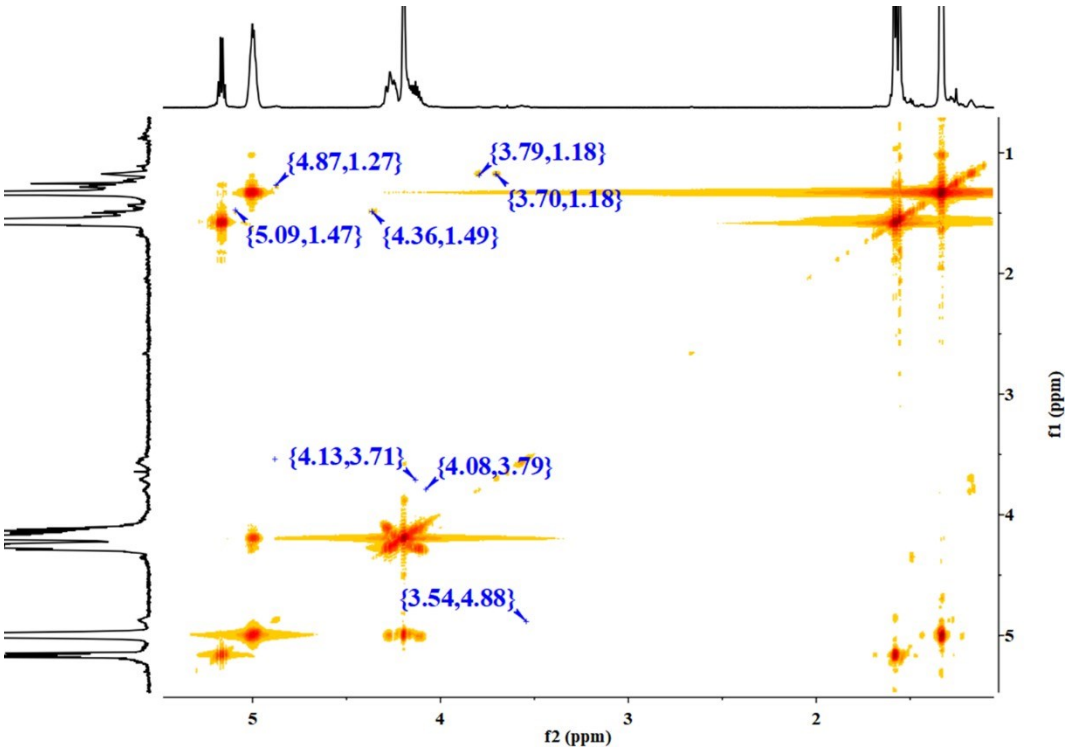

Fig. S5 The HH COSY NMR spectrum of $PLLAPC_2$.

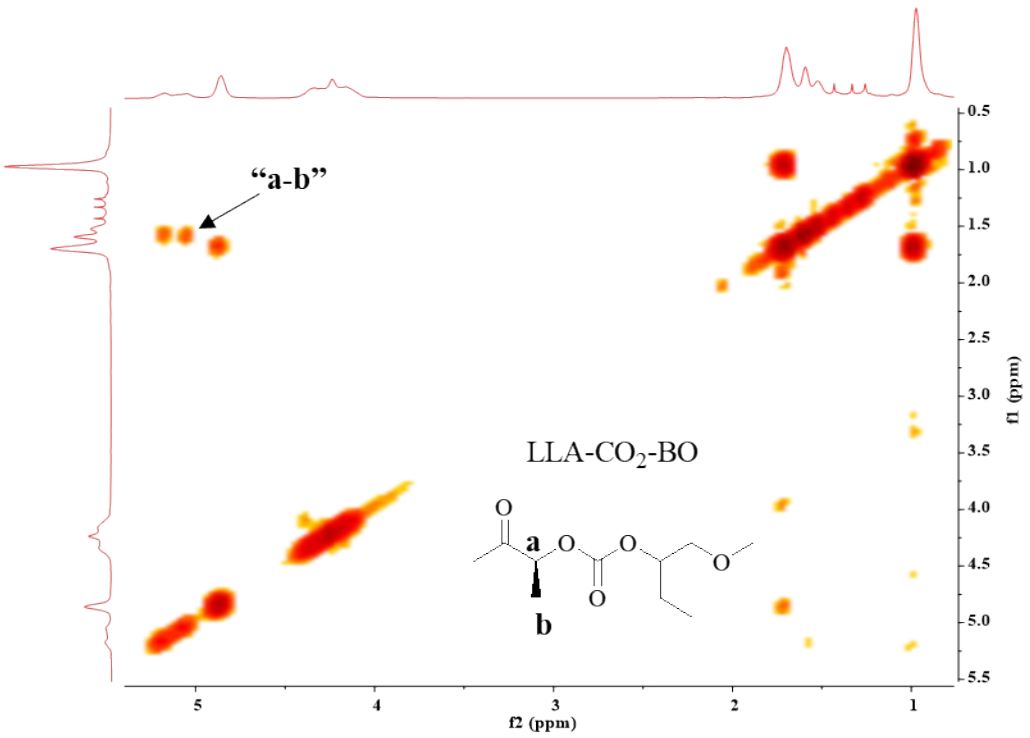

Fig. S6 The HH COSY NMR spectrum of PLLABC$_1$ (Table 2, Entry 17).

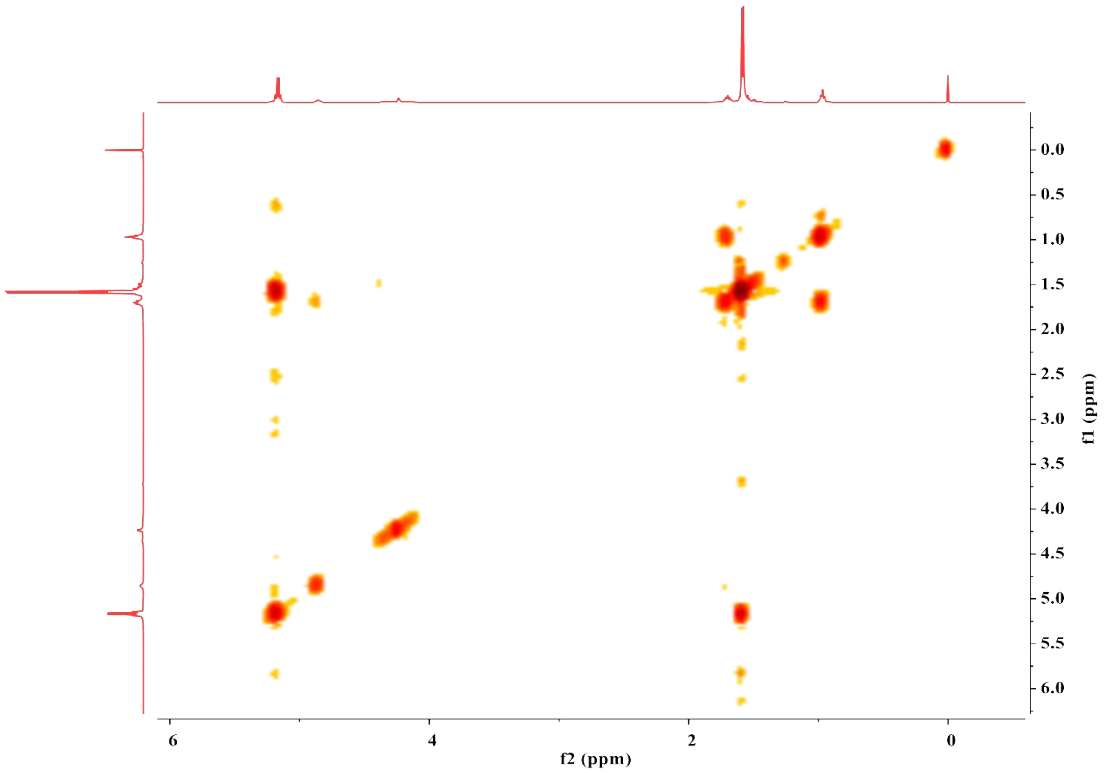

Fig. S7 The HH COSY NMR spectrum of PLLABC$_2$ (Table 2, Entry 18).

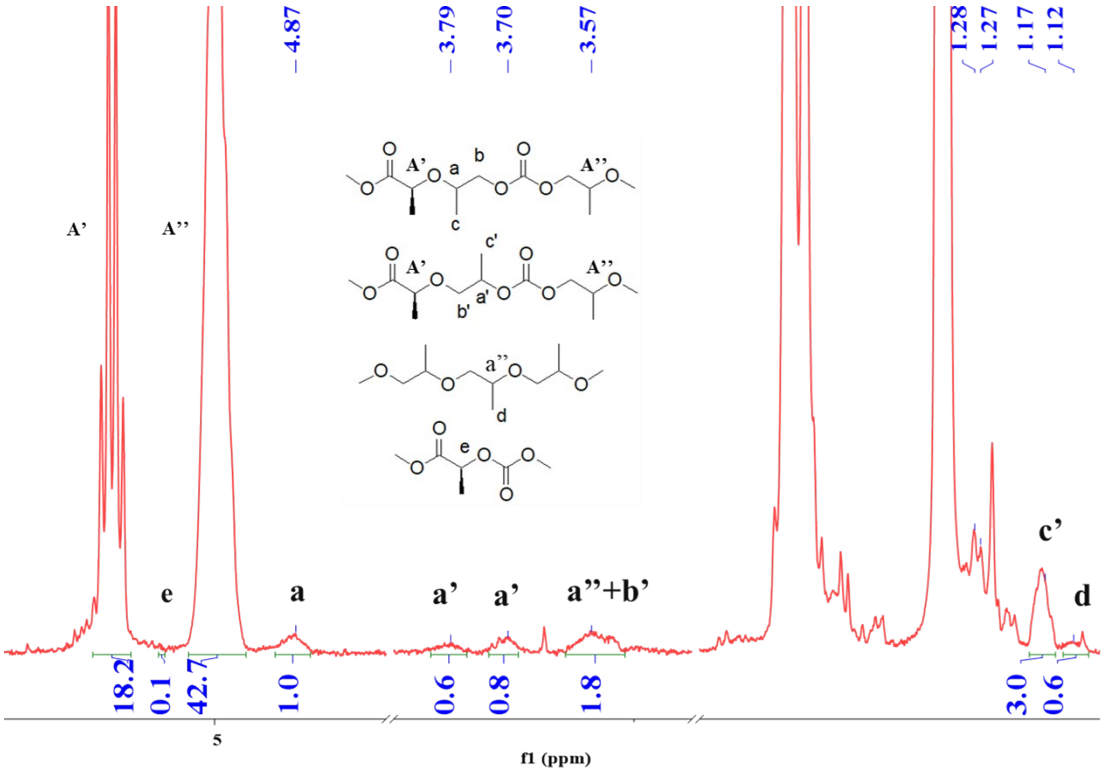

Fig. S8 The ^{1}H NMR spectrum of PLLAPC$_3$ (Table 2, Entry 20).

The average chain length of PPC blocks is 18 [*I*A"/(*I*a+*I*a')], the average chain length of PLLA blocks is 8 [*I*A'/(*I*a+*I*a')]. PLLAPC$_1$has one T_g, while PLLAPC$_2$has two T_gs, one crystal peak and one melting peak (Fig. S9). The thermo-decomposed temperature of PLLAPC$_2$ is 240 ^{o}C, which is higher than PPC$_2$ (219 ^{o}C) (Fig. S10). The mechanical property of PLLAPC$_2$ has been tested in comparison with commercial PLLA resin (Table S2). The dumbbell strip of PLLAPC$_2$ shows slight increase in elongation (from 4% to 6.5%) and decrease in tensile strength (from 65 MPa to 43 MPa).

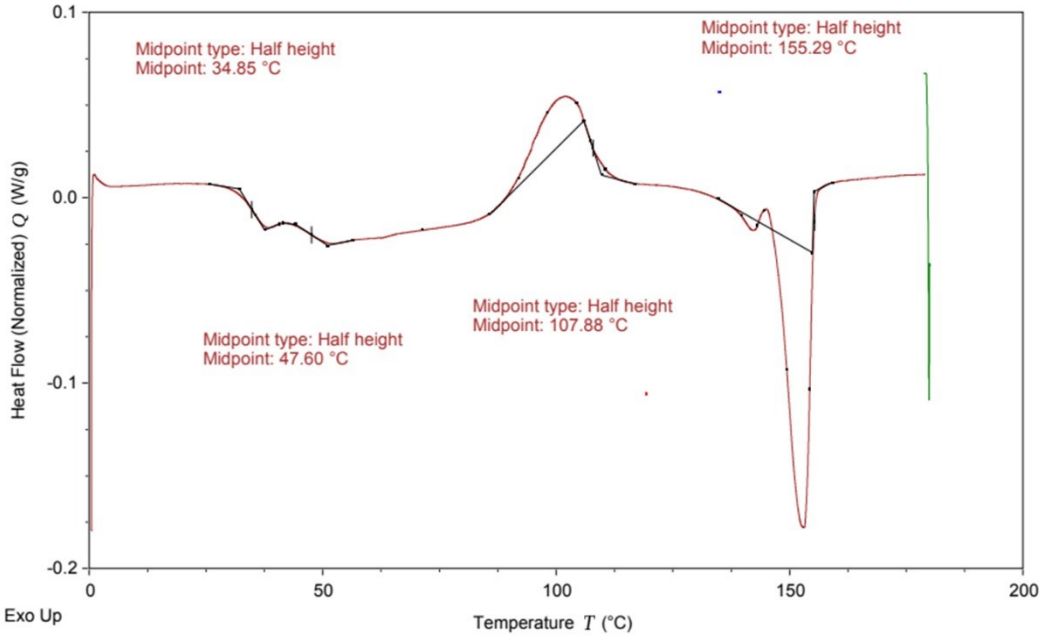

Fig. S9 The DSC curve of PLLAPC$_2$ (Table 2, Entry 16), the second heat route. The PPO content is 6.6%, the average chain length of PPC blocks is 6, the average chain length of PLLA blocks is 9.

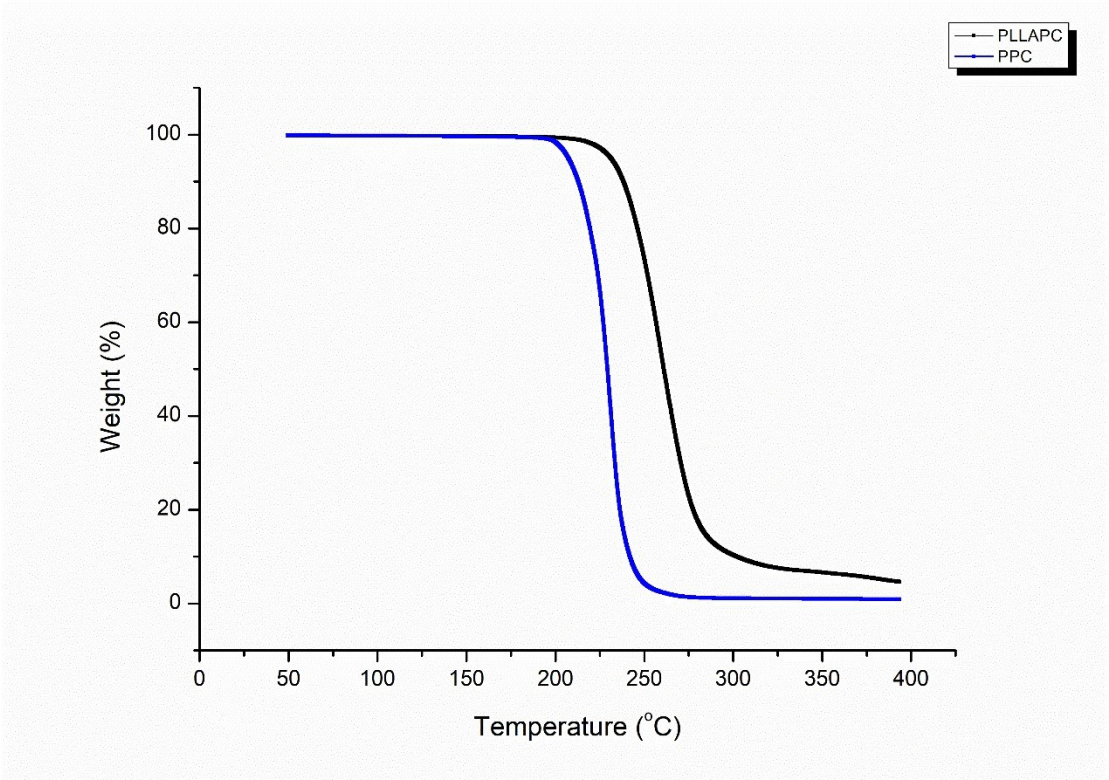

Fig. S10 The TGA curves of PPC_2 and $PLLAPC_2$.

Table S2. Mechanical properties of PLLA and PLLAPC$_2$ (Table 2, Entry 8).

Sample[d]	M_n[a] (Kg/mol)	PDI[a]	EB[b] (%)	TS[c] (MPa)
PLLA	81.2	1.32	4	65
PLLAPC2	602.6	1.02	6.5	43

a. Determined by GPC measurements. b. Elongation at break. c. Tensile strength at yield. d. The average value of five sample.

PLLA, PLLAPC$_2$ were dried at 60 ^{o}C under vacuum for 12 h before use. The tensile properties were measured using an Instron 1211 machine (Instron Co., UK) at a crosshead speed of 20 mm*min^{-1}. The dumbbell-shaped samples for tensile testing were cut from the compression molded sheets, and the dimension of the samples was 20 * 4 * 1 mm^3.

Table S3. The copolymerization of epoxides and CO_2.[a]

Entry	Cat[b]	[Cat]:[PPNCl]:[PO][b]	Time (h)	Conv. (%)[c]	Sel. (%)[d]	M_n[e](Kg/mol)	PDI[e]
1[h]	**1b**	1:1:2500	24	25	38/0[f]	17.8	1.14
2[h]	(**2+1b**)	50:1:2:2500	24	20	34/10[f]	13.2	1.12
3[i]	**2**	1:0:50	19	5	93/0[f]	1.3	1.26
4[i]	(**2+1b**)	50:1:1:1500	23	17	87/0	11.0	1.18

(a) The reactions were performed in 2 mL neat BO or CHO in 25 mL autoclave at 60 °C, 2 MPa CO_2. (b) Molar ratio. (c) Results based on the ^{1}H NMR spectroscopy. (d) Selectivity for polycarbonates over other converted PO, determined by ^{1}H NMR spectroscopy. (e) Determined by gel permeation chromatography, calibrated with polystyrene. (f) Selectivity for polycarbonate/Selectivity for polyether. (g) Under 0.2 MPa CO_2. (h) Using butylene oxide (BO) instead of PO. (i) Using CHO instead of PO.

Table S4. The polymerization of LLA, CHO and CO_2.

Entry	1b[b]	**2**[b]	PPNCl[b]	CHO[b]	LLA[b]	Time (h)	Con. (%)[c]	Sel. (%)[c]
1	1	40	1	2000	150	20 h	53	0
2	-	1	0.05	50	-	20 h	5	0
3	1	100	1	2000	-	20 h	67	0

(a)The reactions were performed in 2 mL neat PO in 25 mL autoclave at 60 °C, 2 MPa CO_2. (b) Molar ratio. (c)Results based on the ^{1}H NMR spectroscopy. Con.: the ratio of converted CHO; Sel.: polyether over other converted CHO.

Interestingly, different epoxides may undergo different paths for copolymerization of LLA, epoxide and CO_2 even using the same TCS_2. The copolymerization of butylene oxide (BO) and CO_2 shows similar results as PO and CO_2 (Table S3, Entries 1 and 2). However, when we used CHO instead of PO, neither ZnGA nor TCS_2 could catalyze the sequential ROP of CHO (Table S4, Entries 2 and 3). As the structure of $PLLAPC_2$ and $PLLABC_2$ is similar, it was believed that they are synthesized via same copolymerization mechanism (Fig. 3). PO and BO are terminal epoxides, by contrast, CHO is internal epoxide. The experiments that using CHO instead of PO show different results, ZnGA or TCS_2 could not catalyze the sequential ROP of CHO (Table S3, Entries 3 and 4), which we suggest is pre-requisite for the synthesis of the "LLA-epoxide-CO_2" linkages. So in the LLA/CHO/CO_2 copolymerization, LLA-CHO-CO_2 linkages could not be synthesized by TCS_2. The $PLLACHC_2$ shows the same microstructure as $PLLACHC_1$, so we regard TCS_2 catalyzed the copolymerization of LLA/CHO/CO_2 via the same way as TCS_1.

Table S5. The polymerization of LLA in PO by ZnGA.

Entry	1b[b]	**2**[b]	PPNCl[b]	PO[b]	LLA[b]	Time (h)	Con.$_1$ (%)[c]	Con.$_2$ (%)[c]	PLA%[c]	M_n[d]	PDI[d]
1	-	100	-	7500	1100	20 h	41	100	42	9400	1.18
2	-	100	1	7500	1100	20 h	7	100	81	7900	1.15
3	1	100	1	3000	450	20 h	22	100	75	12600	1.14
4	1	10	1	3000	450	20 h	20	72	83	10500	1.14
5	1	-	1	2500	250	2 h	-	66	100	5600	1.10

(a)The reactions were performed in 2 mL neat PO in 25 mL autoclave at 60 ^{o}C. (b) Molar ratio. (c)Results based on the ^{1}H NMR spectroscopy, Con.$_1$ is for PO and Con.$_2$ is for LLA. (d) Determined by gel permeation chromatography, calibrated with polystyrene.

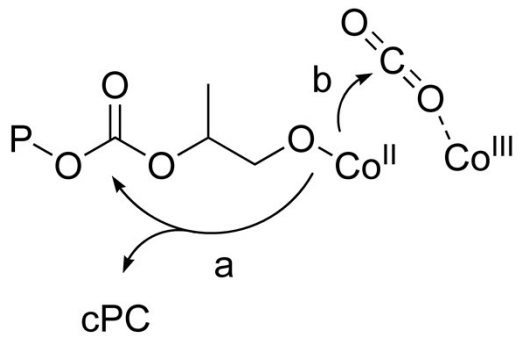

Fig. S11 The “back-biting” reaction (a) and the intermolecular cooperation (b).

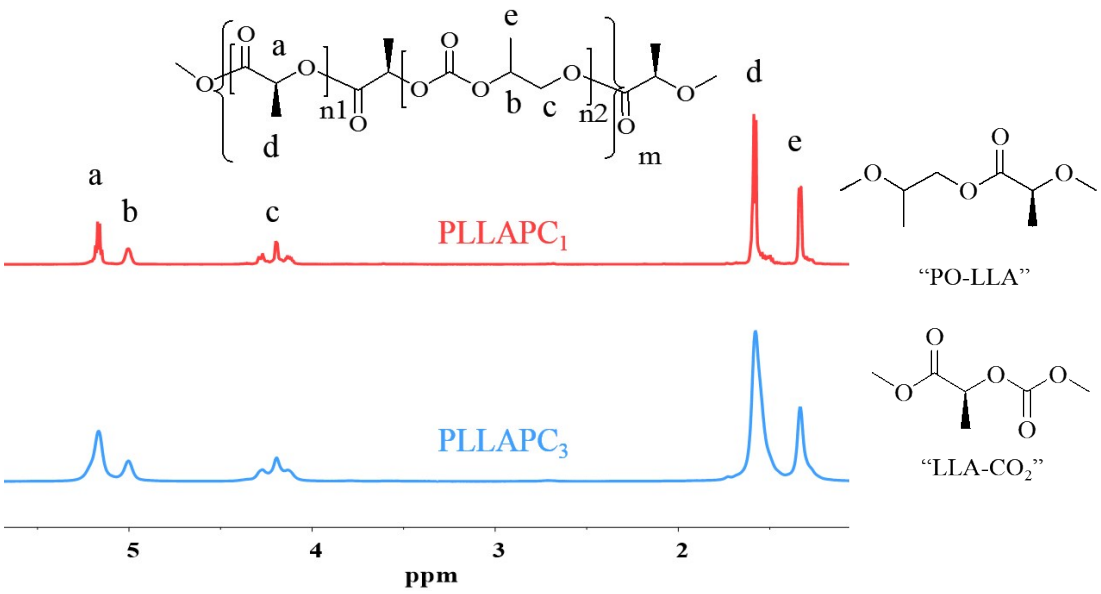

Fig. S12 ^{1}H NMR spectrum of PLLAPC$_1$ (synthesized by TCS$_1$) and PLLAPC$_3$ (synthesized by TCS$_3$).

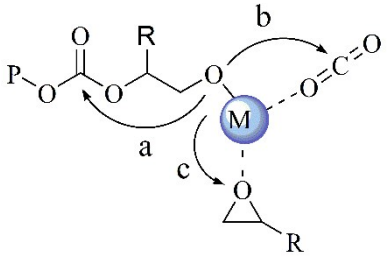

Fig. S13 The catalytic selectivity for epoxide and CO_2 copolymerization.

Table S6. The terpolymerization of PO/LLA/CO_2.[a]

Entry	Cat_1[b]	Cat_2[b]	PPNCl[b]	PO[b]	LLA[b]	Time (h)	Conv.$_1$(%)[c]	Sel.$_1$(%)[c]	Conv.$_2$ (%)[c]	Sel.$_2$ (%)[c]	PLA %[c]	M_n[d]	PDI[d]
1[e]	1	1	1	2500	250	48	50	86	100	0	68	13600	1.40
2[f]	1	1	1	2500	150	20	17	55	95	0	74	8500	1.13
3[g]	1	1	1	2500	150	48	34	12	90	0	-	-	-

(a) The reactions were performed in 2 mL neat PO in 25 mL autoclave at 60 °C, 2 MPa CO_2, employing **1b** as Cat_1. (b) Molar ratio. (c) Results based on the ^{1}H NMR spectroscopy. Con.$_1$ is for PO and Con.$_2$ is for LLA; Sel.1 is for polycarbonates over all converted PO; Sel.$_2$ is for PPO over all converted PO. (d) Determined by gel permeation chromatography, calibrated with polystyrene. (e) Employing **1a** as Cat.2. (f) Employing **2** as Cat.2. (g) Employing **3** as Cat.2.

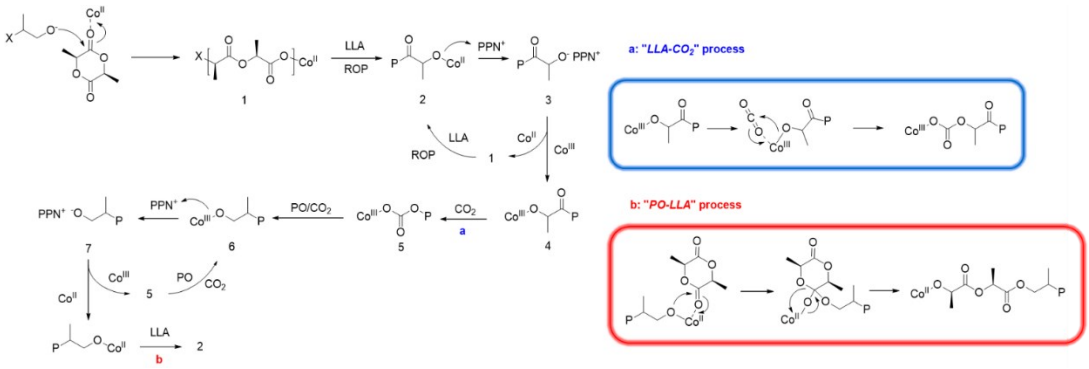

Fig. S14 The conjectural chain propagation circle for TCS1 in previous article.

In our previous work of TCS_1, we suggest that SalenCo^{III} worked for the ROCOP of PO/CO_2, while SalenCo^{II} worked for the ROP of LLA (Fig. S14). The ROP and ROCOP processes are catalyzed simultaneously, and combined by the intermolecular chain transfer. However, this conjecture about the intermolecular cooperation mechanism is not perfect, the synthesis route of "LLA-CO_2" linkage is more complex than we have anticipated. The perception about the copolymerization of LLA/PO/CO_2 is further ameliorated as we investigated more homogeneous ternary catalyst systems. We suggest that SalenCo^{II} could synthesize the "LLA-CO_2" linkage by itself: the growing PLLA chain could directly attack CO_2 on SalenCo^{II}, resulting the formation of "LLA-CO_2" linkage (Fig. S15, step a). When employing SalenCo^{II} (SalenAl or SalenFe) separately in catalyzing the LLA/PO/CO_2 copolymerization, there is a little production of PPC (<0.1%) besides the creation of cPC. Firstly, we regarded the PPC was created by SalenCo^{III}, which is inevitably mixed in the synthesis process of SalenCo^{II}. However, when employing SalenAl or SalenFe, the little creation of PPC was also observed after long reaction time (Table S6). Therefore, we infer that SalenCo^{II} (SalenAl or SalenFe) could synthesize the "LLA-CO_2" linkage by themselves. The growing PLLA chain could directly attack CO_2 on SalenCo^{II} (SalenAl or SalenFe), resulting the formation of "LLA-CO_2" linkage (Fig. S15, step a). Although PO could be ring-opened after the CO_2-insertion step, the following "back-biting" reaction leads to the creation of cPC which prevents SalenCo^{II} to consecutively catalyze the ROCOP of PO/CO_2 (Fig. S15, step c). So the main products are PLLA and cPC when employing SalenCo^{II} (SalenAl or SalenFe). For the ternary catalyst systems, the intermolecular chain transfer would replace the "back-biting" reaction (Fig. S15, step c'), similar as in catalyzing the PO/CO_2 copolymerization (Fig. S13). This suggestion is consistent with that PLLA could not induct the PO/CO_2 copolymerization on SalenCo^{III} as a macroinitiator, and the ROP of LLA would be terminated by the addition of CO_2 (Table S7). As reported, SalenCo^{III} could provide PPO under low pressure CO_2 (Table 1, Entry 4),[2] and SalenCo^{III} could also catalyze the copolymerization of LLA/PO/CO_2 under 0.2 Mpa CO_2 (Table 2, Entry 3), which means TCS_1 could also act via mechanism showed in Fig. 3.

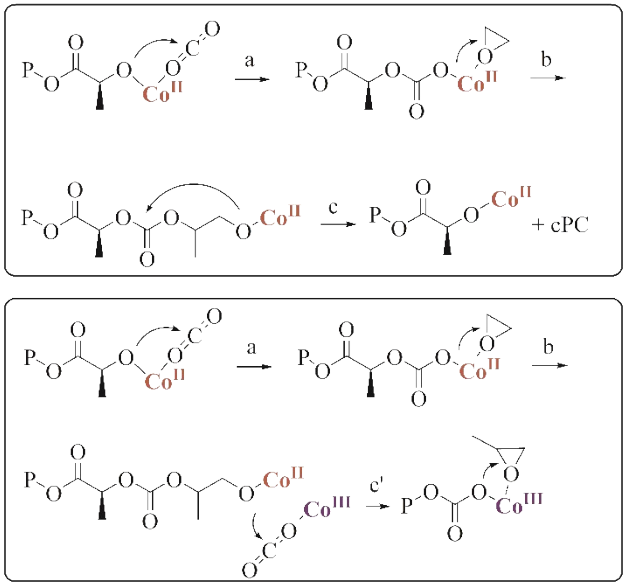

Fig. S15 Revised chain propagation circle for TCS_1 in catalyzing the copolymerization of LLA, PO and CO_2.

Table S7. The copolymerization of LLA, PO and CO_2.[a]

Entry	Cat.[b]	[Cat]:[PPNCl]:[PO]:[LLA][b]	Time (g)	$Con._{PO}$ (%)[c]	Sel. (%)[c]	$Con._{LLA}$ (%)[c]
1	3a	1:1:4000:400	48	8	61	95
2	3b	1:1:2500:250	48	4	25	95

(a) The reactions were performed in 2 mL neat PO in 5 mL autoclave at 60 °C, 2 MPa CO_2, employing **1b** as Cat_1. (b) Molar ratio. (c) Results based on the ^{1}H NMR spectroscopy. Sel. is for polycarbonates over all converted PO.

Table S8. The polymerization of LLA.

Step	Cat[b]	PPNCl[b]	PO[b]	LLA[b]	Time (h)	Con.$_1$ (%)[c]	Sel. (%)[c]	Con.$_2$ (%)[c]
1	1	1	3500	350	6	-	-	47
2[d]	1	1	3500	350	18	-	-	47

(a) The reactions were performed in 2 mL neat PO in 5 mL autoclave at 60 ^{o}C, employing **1b** as Cat. (b) Molar ratio. (c) Results based on the ^{1}H NMR spectroscopy. Con.$_1$ is for PO and Con.$_2$ is for LLA; Sel. is for polycarbonates over all converted PO. (d) Adding 2 MPa CO_2.

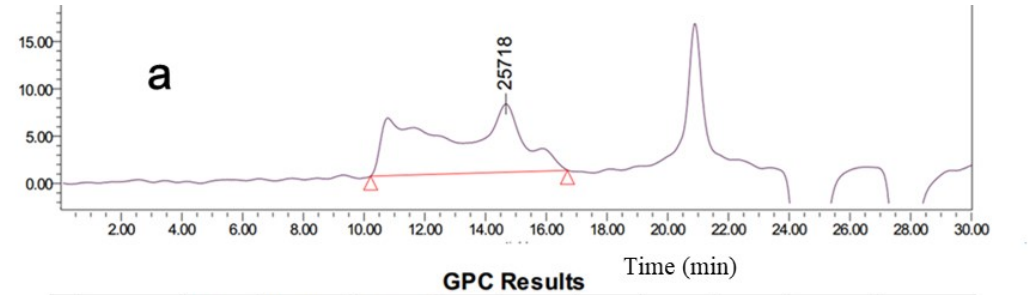

GPC Results

	Dist Name	Elution Volume (ml)	Retention Time (min)	Adjusted RT (min)	Mn	Mw	MP	Mz	Mz+1	Mz/Mw	Mz+1/Mw
1		14.669	14.669	14.669	40624	134902	25718	308316	410885	2.285483	3.045811

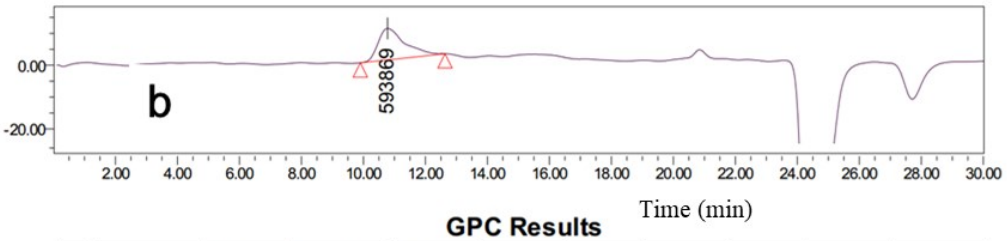

GPC Results

	Dist Name	Elution Volume (ml)	Retention Time (min)	Adjusted RT (min)	Mn	Mw	MP	Mz	Mz+1	Mz/Mw
1		10.779	10.779	10.779	339714	393525	593869	436822	468796	1.110022

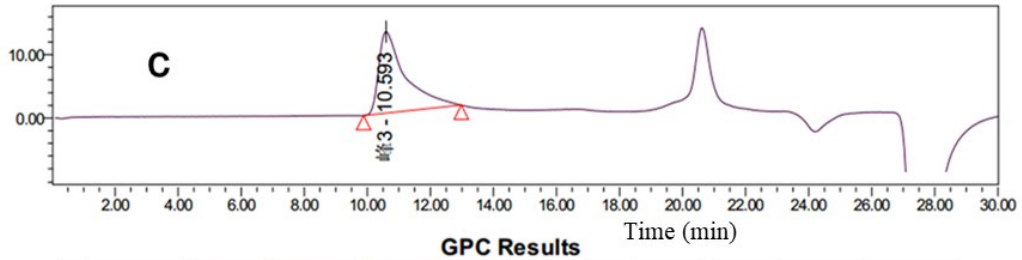

GPC Results

	Dist Name	Elution Volume (ml)	Retention Time (min)	Adjusted RT (min)	Mn	Mw	MP	Mz	Mz+1	Mz/Mw	Mz+1/Mw
1		10.593	10.593	10.593	322125	379639		428369	465181	1.128360	1.225325

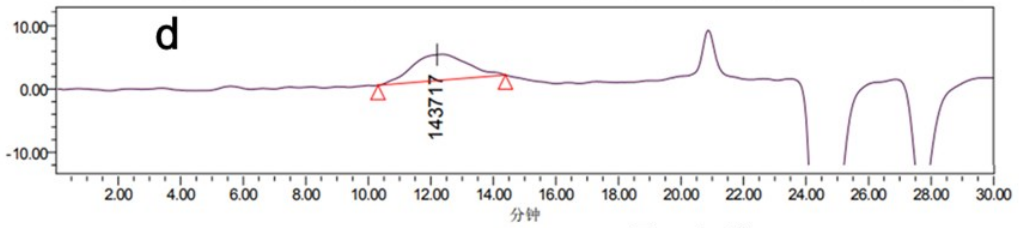

GPC Results

	Dist Name	Elution Volume (ml)	Retention Time (min)	Adjusted RT (min)	Mn	Mw	MP	Mz	Mz+1	Mz/Mw
1		12.209	12.209	12.209	110907	164661	143717	237092	312449	1.439878

Fig. S16 The GPC curves in CH_2Cl_2, a: mixture, b, c, and d: $PLLAPC_2$.

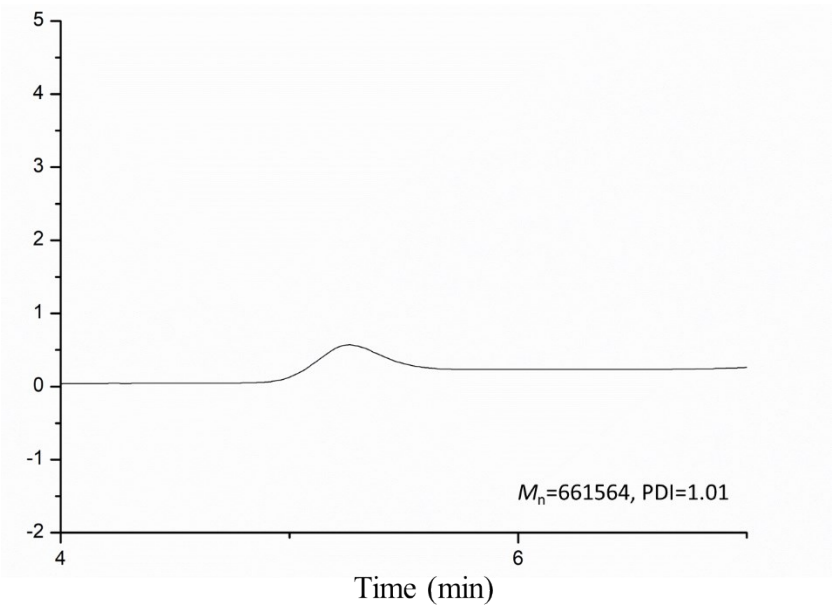

Fig. S17 The GPC curve in THF (Table 2, Entry 11) .

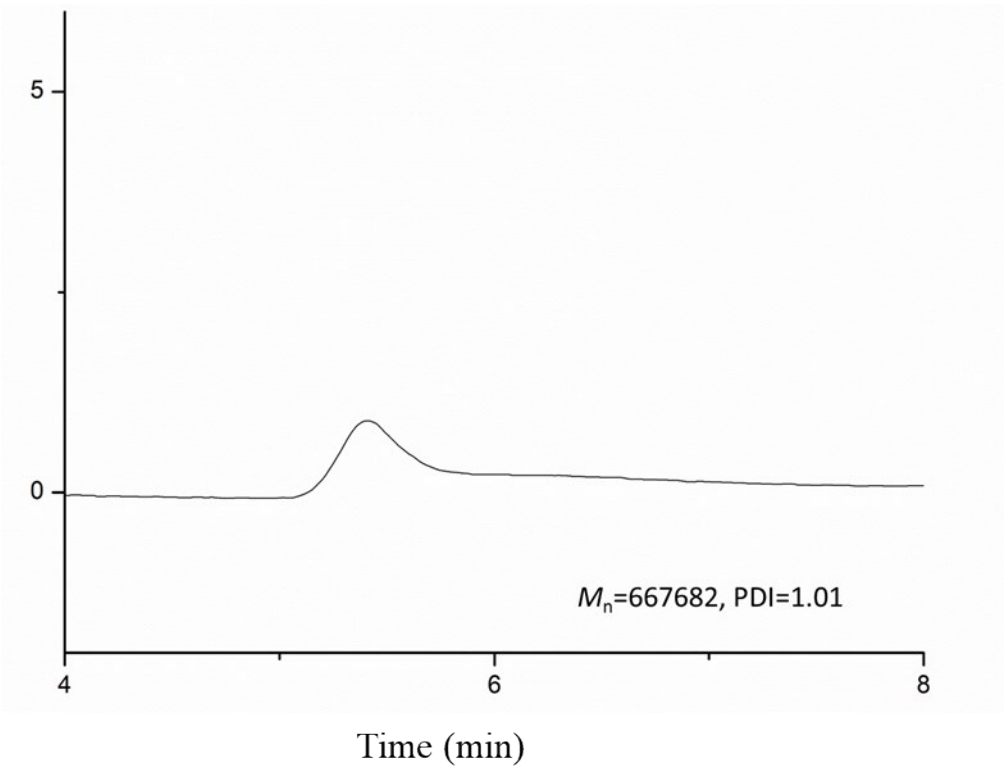

Fig. S18 The GPC curve in THF (Table 2, Entry 11).

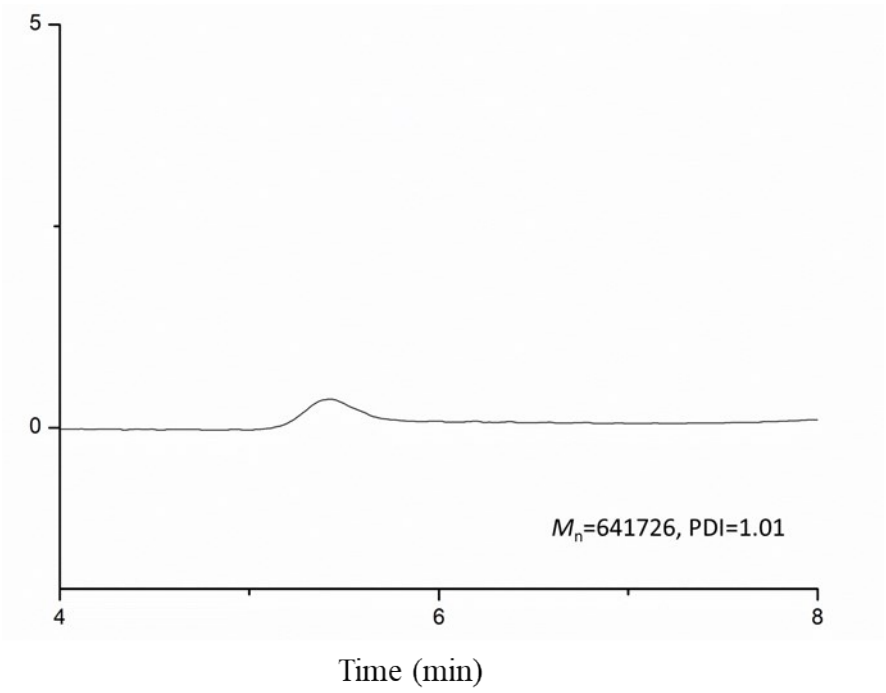

Fig. S19 The GPC curve in THF (Table 2, Entry 9).

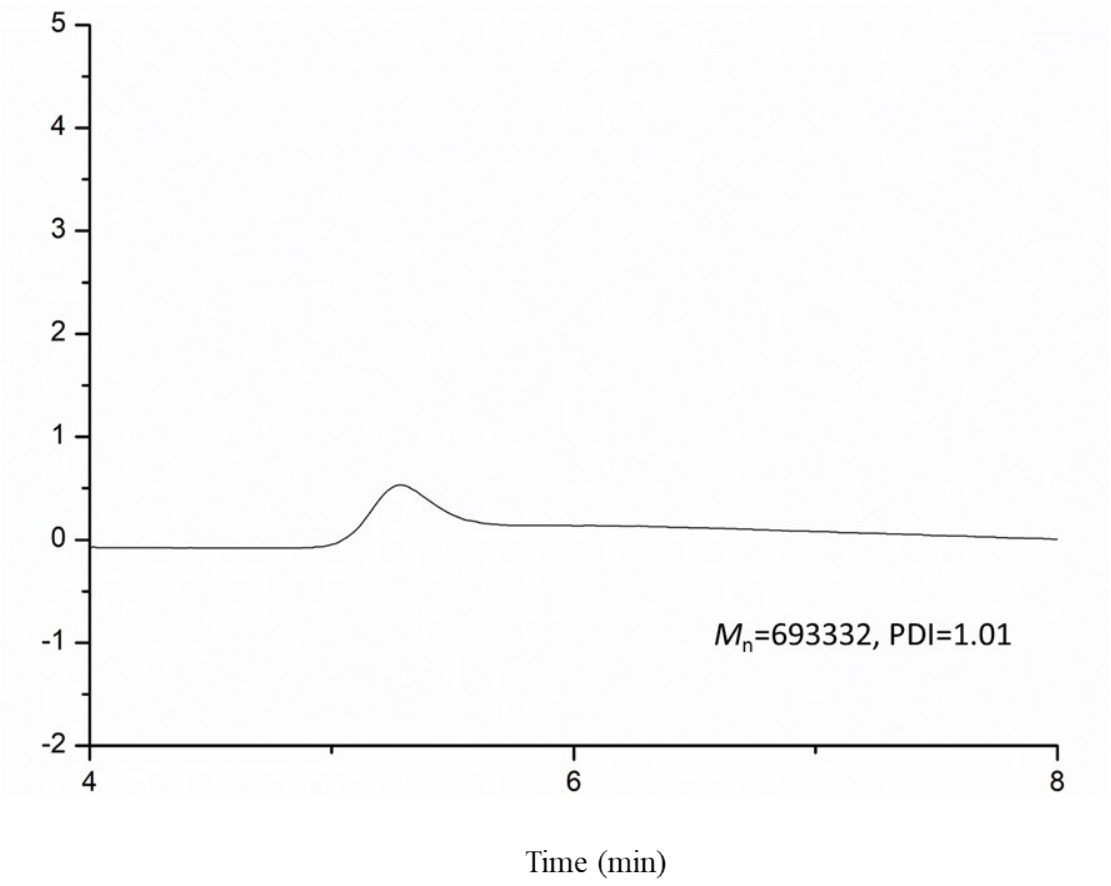

Fig. S20 The GPC curve in THF (Table 2, Entry 9).

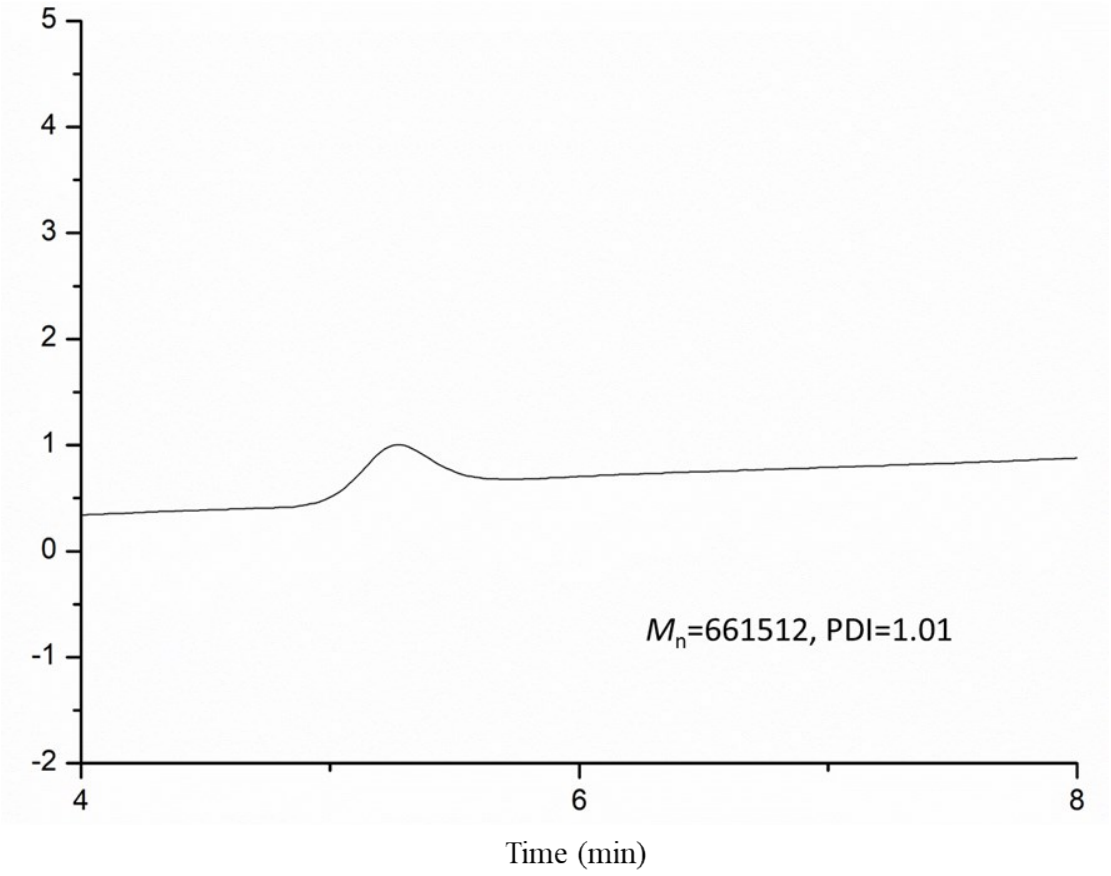

Fig. S21 The GPC curve in THF (Table 2, Entry 11).

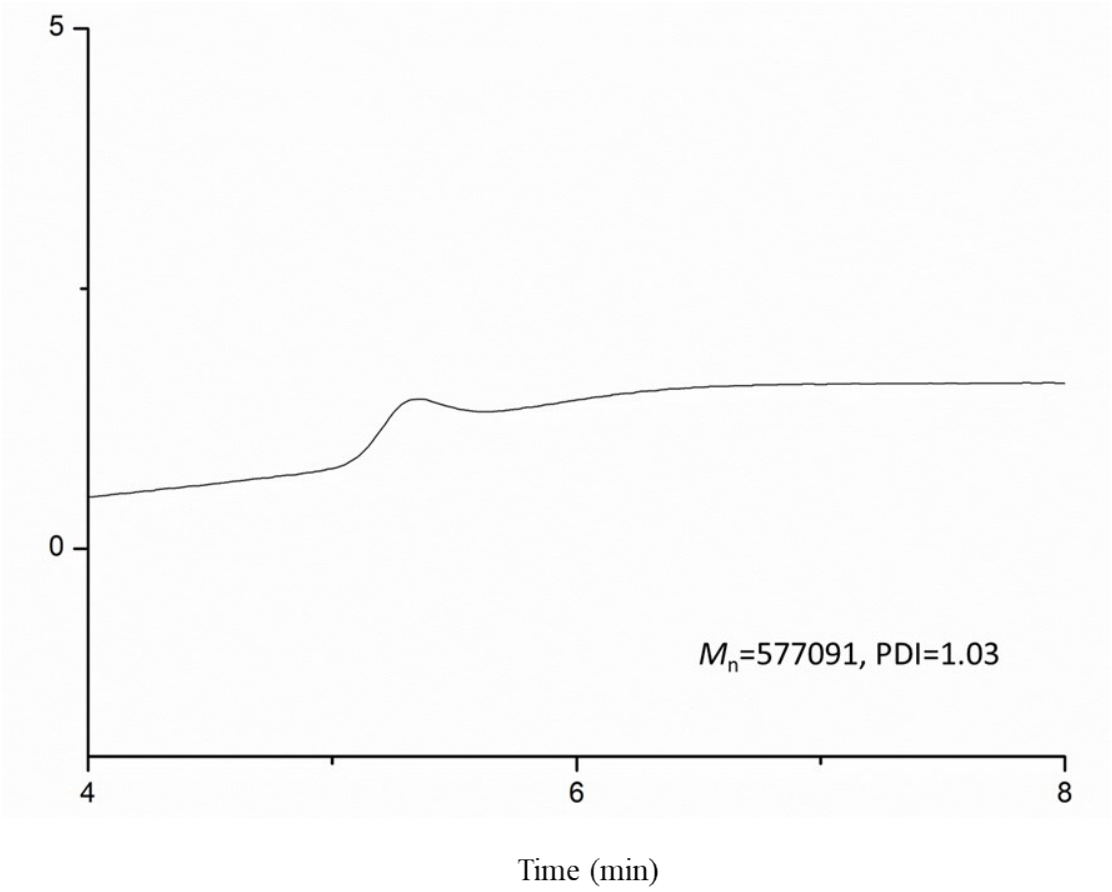

Fig. S22 The GPC curve in THF (Table 2, Entry 12).

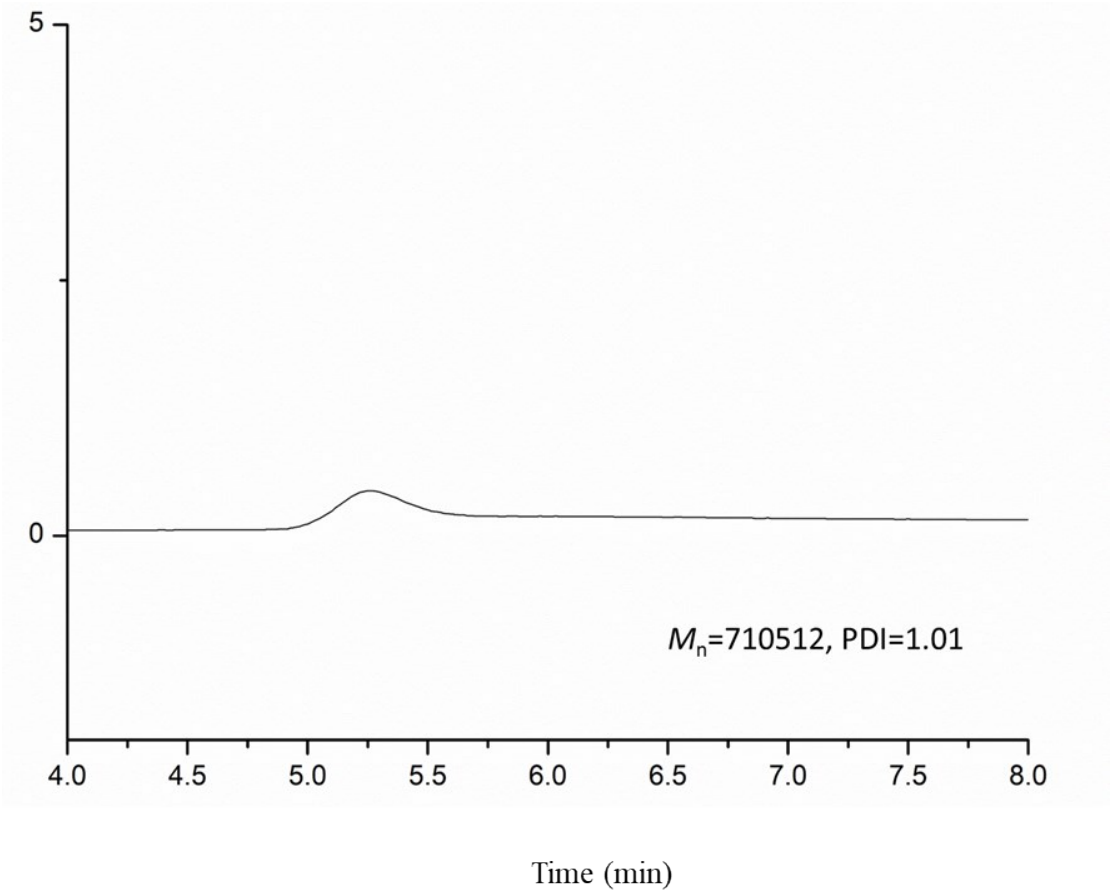

Fig. S23 The GPC curve in THF (Table 2, Entry 7).

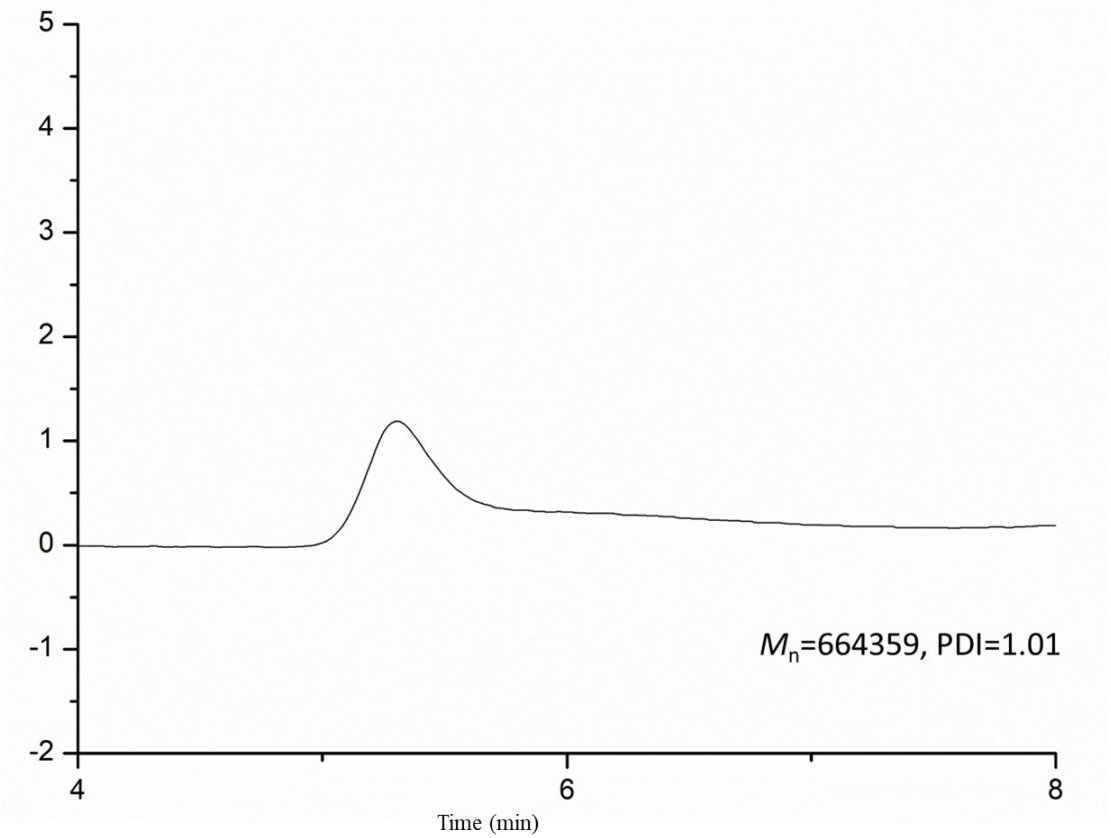

Fig. S24 The GPC curve in THF (Table 2, Entry 11).

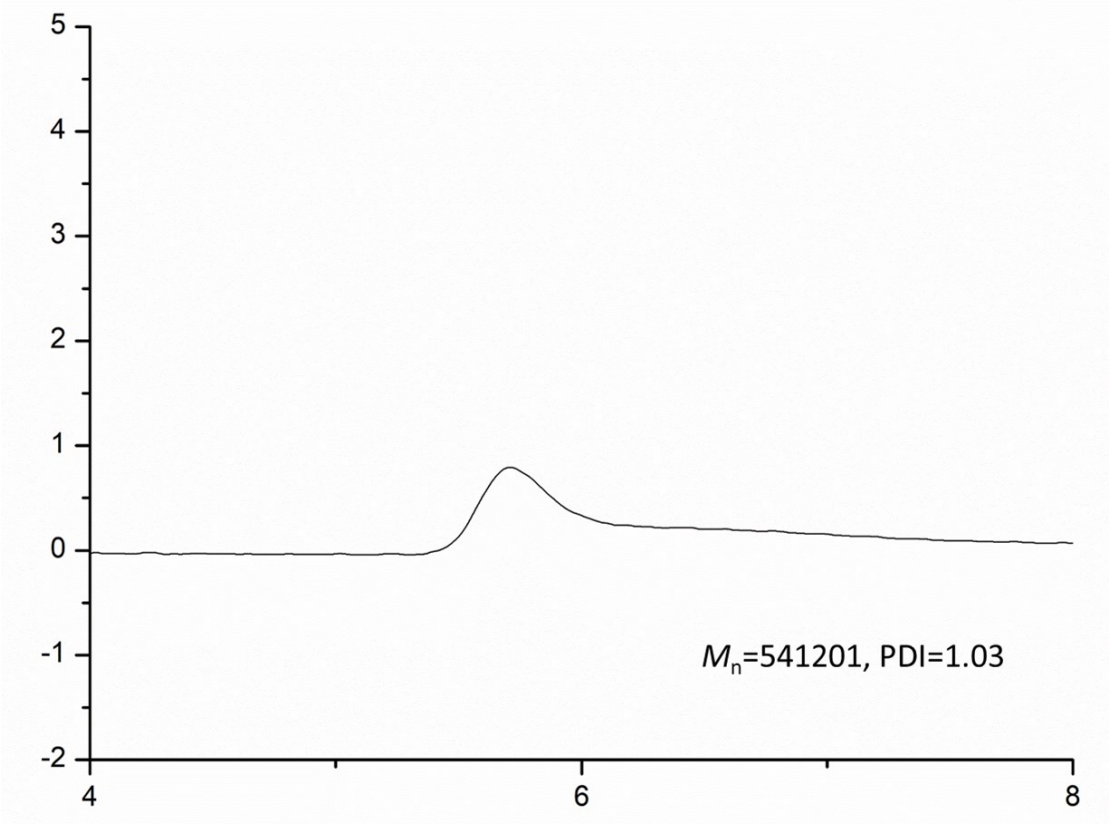

Fig. S25 The GPC curve in THF (Table 2, Entry 13).

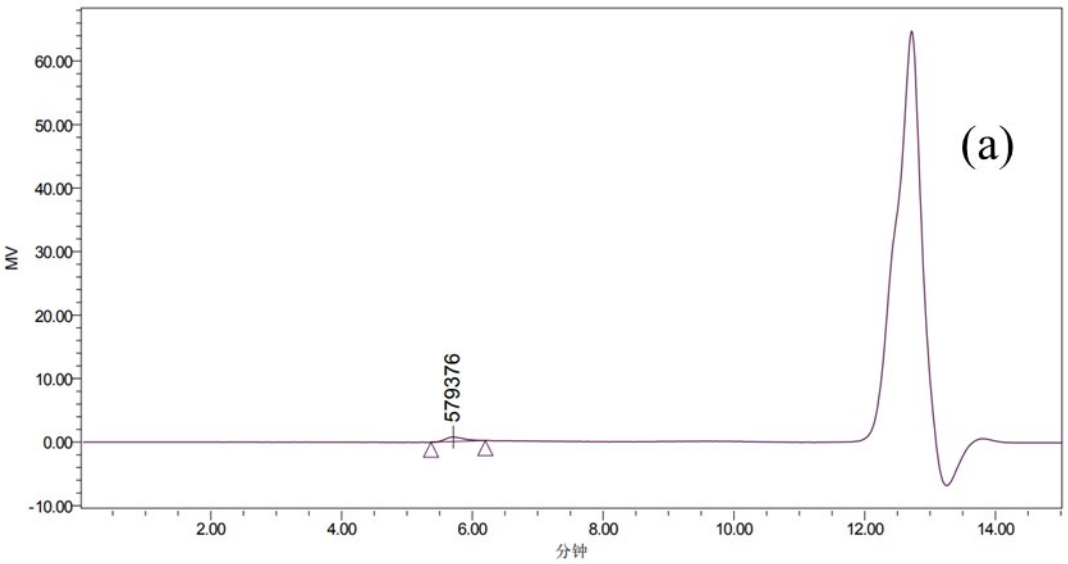

宽分布未知样相对峰表

	分布名	Mn (道尔顿)	Mw (道尔顿)	MP	Mz (道尔顿)	Mz+1 (道尔顿)	多分散性	Mz/Mw	Mz+1/Mw
1		541201	555173	579376	568359	580653	1.025817	1.023751	1.045895

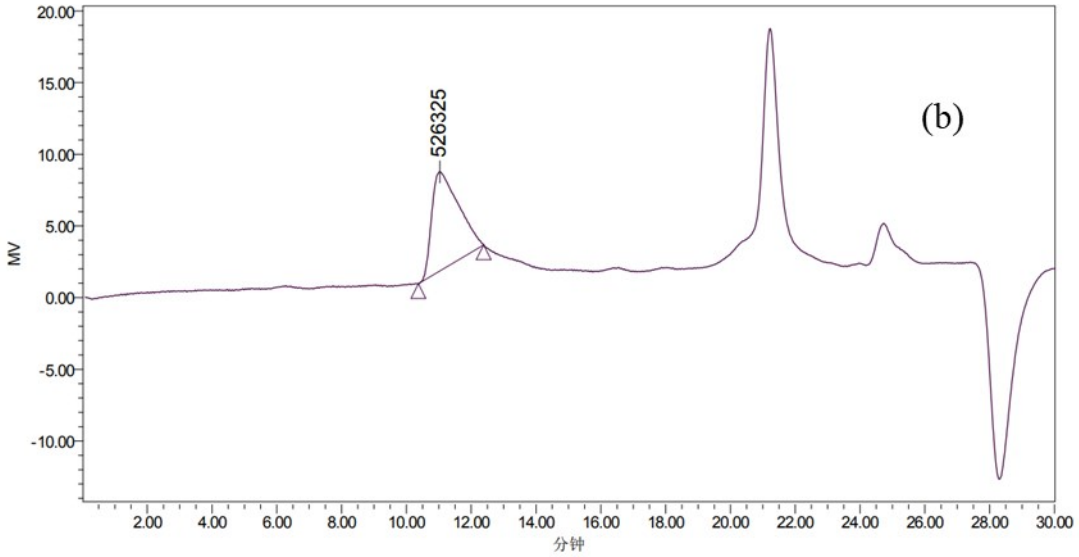

宽分布未知样相对峰表

	分布名	Mn (道尔顿)	Mw (道尔顿)	MP	Mz (道尔顿)	Mz+1 (道尔顿)	多分散性	Mz/Mw	Mz+1/Mw
1		336088	375577	526325	411069	440331	1.11749€	1.094499	1.172409

Fig. S26 The GPC curve in THF (a) and CH_2Cl_2 (b) (Table 2, Entry 13).

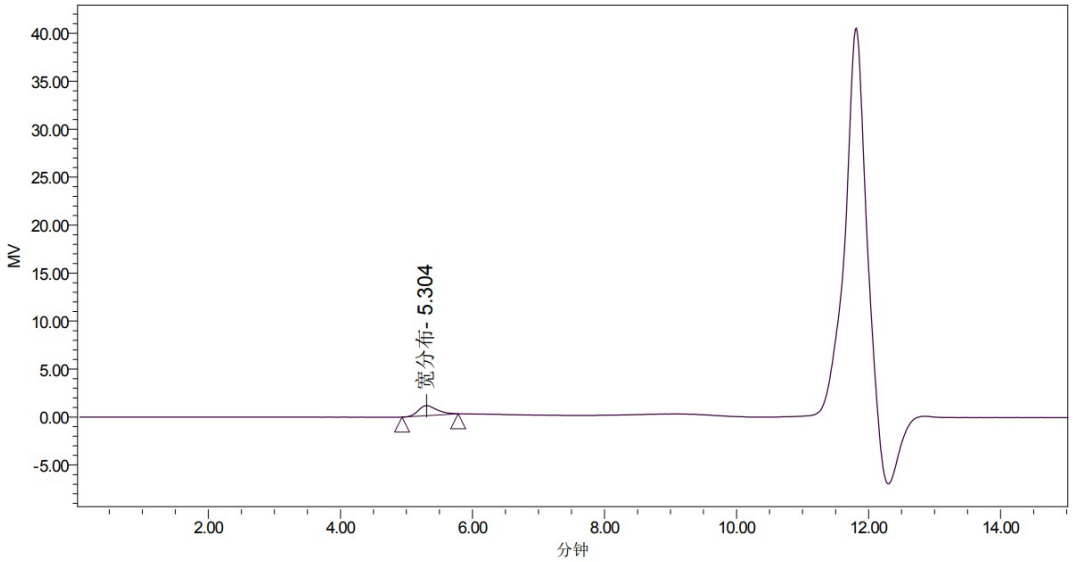

宽分布未知样相对峰表

	分布名	Mn (道尔顿)	Mw (道尔顿)	MP	Mz (道尔顿)	Mz+1 (道尔顿)	多分散性	Mz/Mw	Mz+1/Mw
1		664359	667855		671174	674313	1.005262	1.004970	1.009670

Fig. S27 The GPC curve in THF (Table 2, Entry 11).

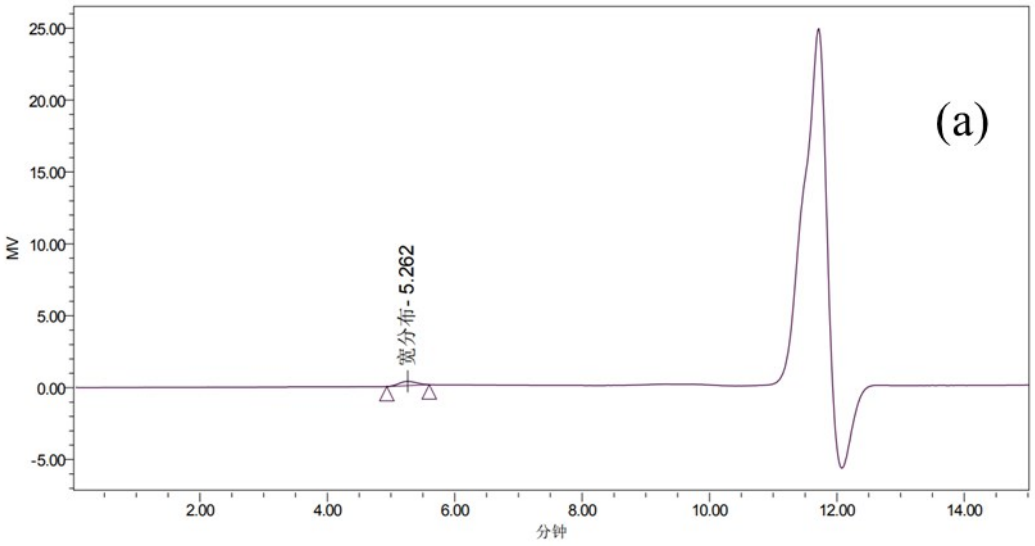

宽分布未知样相对峰表

	分布名	Mn (道尔顿)	Mw (道尔顿)	MP	Mz (道尔顿)	Mz+1 (道尔顿)	多分散性	Mz/Mw	Mz+1/Mw
1		710512	710823		71113(	711432	1.000438	1.000432	1.000857

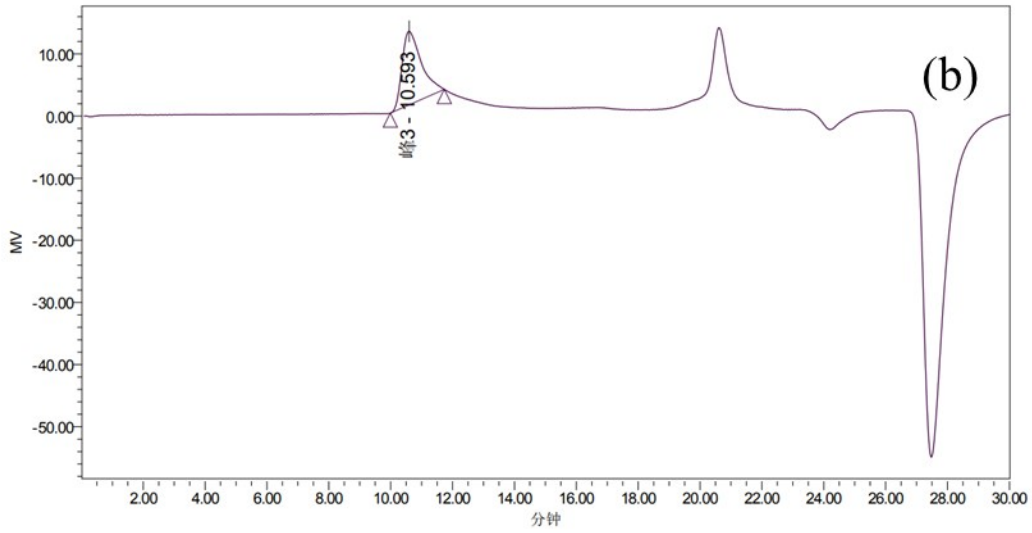

宽分布未知样相对峰表

	分布名	Mn (道尔顿)	Mw (道尔顿)	MP	Mz (道尔顿)	Mz+1 (道尔顿)	多分散性	Mz/Mw	Mz+1/Mw
1		456203	475853		493079	507710	1.043073	1.036202	1.066948

Fig. S28 The GPC curve in THF (a) and CH_2Cl_2 (b) (Table 2, Entry 9).

REFERENCES

(1). Zhang, B.; Bian, X.; Zhou, D.; Feng, L.; Li, G.; Chen, X. *Rsc Adv.*, 2016, **6**, 113366-113376.

(2). Li, X.; Duan, R.; Pang, X.; Gao, B.; Wang, X.; Chen, X. *Appl. Catal., B*. 2016, **182**, 580-586.